Compact source of narrow-band counterpropagating polarization-entangled photon pairs using a single dual-periodically-poled crystal

Yan-Xiao Gong,[1,2] Zhen-Da Xie,[2] Ping Xu,[2,*] Xiao-Qiang Yu,[1] Peng Xue,[1] and Shi-Ning Zhu[2]

[1]*Department of Physics, Southeast University, Nanjing 211189, People's Republic of China*

[2]*National Laboratory of Solid State Microstructures and School of Physics, Nanjing University, Nanjing 210093, People's Republic of China*

(Received 30 August 2011; published 14 November 2011)

We propose a scheme for the generation of counterpropagating polarization-entangled photon pairs from a dual-periodically-poled crystal. Compared with the usual forward-wave-type source, this source, in the backward-wave way, has a much narrower bandwidth. With a 2-cm-long bulk crystal, the bandwidths of the example sources are estimated to be 3.6 GHz, and the spectral brightnesses are more than 100 pairs/(s GHz mW). Two concurrent quasi-phase-matched spontaneous parametric down-conversion processes in a single crystal enable our source to be compact and stable. This scheme does not rely on any state projection and applies to both degenerate and nondegenerate cases, facilitating applications of the entangled photons.

DOI: 10.1103/PhysRevA.84.053825 PACS number(s): 42.65.Lm, 42.50.Dv, 03.67.Bg

I. INTRODUCTION

Polarization-entangled photons play a key role not only in testing the foundations of quantum mechanics [1] but also in various photonic quantum technologies [2]. A compact, robust, and high-brightness source of polarization-entangled photons is therefore desirable for practical implementation of a variety of entanglement-based applications.

Spontaneous parametric down-conversion (SPDC) in nonlinear crystals is a successful technique to generate polarization-entangled photon pairs. A typical method involves using the type-II birefringence phase-matching (BPM) in a nonlinear crystal [3], such as beta barium borate (BBO). However, only a small fraction of the total emitted photons, the intersecting locations of two nonoverlapping cones, are polarization-entangled, and therefore such a source is inefficient. A more efficient source consists of two type-I nonlinear crystals via BPM [4,5], from which polarization-entangled photons are emitted in a cone. However, generally only a small fraction of the cone is collected for use, and thus such a source is again less efficient.

One way to solve the inefficiency problem in the conelike sources is by means of quasi-phase-matching (QPM) [6,7] in periodically poled (PP) crystals [8], such as periodically poled lithium niobate (PPLN) and periodically poled potassium titanyl phosphate (PPKTP). QPM has advantages over BPM due to its higher efficiency and the fact that it enables flexible frequency-tunable processes. In particular, QPM enables the collinear and beamlike configuration of the photon pairs. Consequently, it is possible to make a much bigger fraction of the created photons polarization-entangled rather than conelike sources, thus leading to more efficient sources. However, a new problem arises, namely the need to spatially separate the collinear photon pairs.

A simple method to solve this problem is by using dichroic mirrors when the photon pairs are generated at substantially different frequencies. In this way, several nondegenerate polarization entanglement sources have been designed by coherently combining two SPDC sources at a polarizing beam splitter [9–15], by manipulating polarization ququarts [16], by overlapping two cascaded PP crystals [17,18], or by two cascaded [19] or concurrent [20,21] SPDC processes in a single PP crystal. These nondegenerate sources have various applications, such as, for instance, in quantum communication [22]. However, in many entanglement-based applications, such as, for example, in quantum computation [23], frequency-degenerate polarization-entangled photons are required. A straightforward way to build degenerate entangled sources based on PP crystals is by separating collinear orthogonally polarized photon pairs with a beam splitter followed by twofold coincidence measurement as a postselection [24]. However, this method suffers a 50% loss. A postselection-free method employs interferometers to combine two pairs of orthogonally polarized photons [25,26], but such interferometric sources (also the nondegenerate sources in Refs. [9–15]) require stringent phase control and stabilization.

Another problem of SPDC sources lies in the broad bandwidth determined by the phase-matching condition, which is usually on the order of several THz or hundreds of GHz. The broadband SPDC source becomes very dim in many applications requiring narrow-band photons, such as long-distance fiber optical quantum communication (∼GHz [27]), strong interaction of the photons with atoms and molecules(∼MHz [28], and recently relaxed to several GHz [29,30]), and interference of independent sources without time synchronization (∼GHz [31]). Passive filtering is a straightforward way to obtain narrow-band sources [27,31], but it will greatly reduce the generation rate. Cavity-enhanced SPDC can provide high-brightness narrow-band photon paris [32–34]. However, additional spectral filtering is required to obtain single-mode output due to the broad gain bandwidth.

In this paper, we succeed in solving all the above problems by building a compact and narrow-band polarization-entanglement source based on the backward-wave-type SPDC in a dual-periodically-poled crystal. The backward-wave-type SPDC [35–37] has a much narrower bandwidth than the forward-wave interaction. The counterpropagating photon pair generation has also been extensively studied in waveguide structures [38–41]. Moreover, it not only has the same advantage as the usual collinear, beamlike output SPDC on photon collection and overlapping for possible polarization

*pingxu520@nju.edu.cn

entanglement, but it also does not suffer from the problem of spatial separation. Our scheme relies on the coherence of two concurrent backward-wave-type SPDC processes in a single PP crystal, rather than any interferometer and post-selection. Furthermore, this scheme can work in frequency-degenerate and -nondegenerate cases, for which we design two experimentally feasible structures, respectively. With a 2-cm-long bulk crystal, the bandwidths of the two sources are estimated to be 3.6 GHz, with spectral brightnesses of 115 and 154 pairs/(s GHz mW), respectively.

The rest of this paper is organized as follows. In the next section, we give a description of the dual-periodically-poled crystal and design the structures required in our scheme. In Sec. III, we introduce our scheme and make detailed calculations on the sources we propose. Section IV contains our conclusions.

II. DESCRIPTION OF A DUAL-PERIODICALLY-POLED CRYSTAL

QPM originates from modulation of the second-order nonlinear susceptibility $\chi^{(2)}$. It has been advanced to a variety of domain structures that allow multiple and flexible nonlinear processes in a single crystal, leading to compact and integrated devices. A dual-periodic structure is one of the QPM structures that permits two coupled optical parametric interactions [42,43]. Here, taking the potassium titanyl phosphate (KTP) crystal as an example, we design a dual-periodic structure to satisfy two concurrent SPDC processes, $H_p \rightarrow H_s + V_i$ and $H_p \rightarrow V_s + H_i$, where p, s, and i represent the pump, signal, and idler fields, respectively, with H (V) denoting the horizontal (vertical) polarization.

The schematic of a dual-periodically-poled KTP (DPPKTP) crystal is shown in Fig. 1, in which inverted domains (with $-\chi^{(2)}$) distribute on a $+\chi^{(2)}$ background as a dual-periodic structure. It is formed by twice-periodic modulation of $\chi^{(2)}$. Suppose $g_1(x)$ and $g_2(x)$ are two periodic functions as the sign of nonlinearity $\chi^{(2)}$. Then their Fourier expansions can be written as

$$g_1(x) = \sum_m \mathcal{G}_m e^{-iG_m x}, \tag{1}$$

$$g_2(x) = \sum_n \mathcal{G}_n e^{-iG_n x}, \tag{2}$$

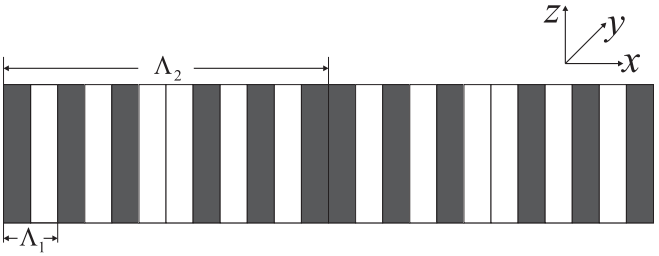

FIG. 1. Schematic of a dual-periodically-poled potassium titanyl phosphate crystal. Gray and blank areas are inverted ($-\chi^{(2)}$) and background positive ($\chi^{(2)}$) domains, respectively.

respectively, where the reciprocals are

$$G_m = \frac{2m\pi}{\Lambda_1}, \quad G_n = \frac{2n\pi}{\Lambda_2}, \tag{3}$$

and the Fourier coefficients

$$\mathcal{G}_m = \frac{2}{m\pi}\sin(mD_1\pi), \quad \mathcal{G}_n = \frac{2}{n\pi}\sin(nD_2\pi), \tag{4}$$

with Λ_1 and Λ_2 ($\Lambda_1 < \Lambda_2$) denoting the two modulation periods, D_1 and D_2 representing the duty cycles, and nonzero integers m and n indicating the orders of reciprocals. Then we can write the dual-periodic structure as

$$g(x) = g_1(x)g_2(x) = \sum_{m,n} \mathcal{G}_{m,n} e^{-iG_{m,n}x}, \tag{5}$$

where

$$\mathcal{G}_{m,n} = \mathcal{G}_m\mathcal{G}_n = \frac{4}{mn\pi^2}\sin(mD_1\pi)\sin(nD_2\pi), \tag{6}$$

$$G_{m,n} = G_m + G_n = \frac{2m\pi}{\Lambda_1} + \frac{2n\pi}{\Lambda_2}. \tag{7}$$

Then the modulation of the second-order nonlinear susceptibility $\chi^{(2)}$ can be described as

$$\chi^{(2)}(x) = dg(x) = d\sum_{m,n} \mathcal{G}_{m,n} e^{-iG_{m,n}x}, \tag{8}$$

where d is the effective nonlinear coefficient.

An arbitrary twice-periodic modulation could result in smaller domains, which may make fabrication more difficult. A straightforward way to avoid the unwanted small domains is by designing the structure such that

$$\begin{aligned} \Lambda_2/\Lambda_1 &= l/2, \\ D_1 &= 1/2, \\ D_2 &= \lfloor l/2 \rfloor / l, \quad \text{where } l \text{ is an integer bigger than 2}, \end{aligned} \tag{9}$$

where $\lfloor\cdot\rfloor$ is the floor function to get the integer part of a number. In practice, this condition can be satisfied by tuning the temperature and wavelengths.

We consider the pump wave vector along the x direction and H (V) in the y (z) directions. By choosing the right wavelengths and temperature, we are able to obtain the following QPM conditions for two backward-wave-type SPDC processes:

$$\Delta k_1 = k_{p,H} - k_{s,H} + k_{i,V} - G_{m_1,n_1} = 0, \tag{10}$$

$$\Delta k_2 = k_{p,H} - k_{s,V} + k_{i,H} - G_{m_2,n_2} = 0, \tag{11}$$

where G_{m_1,n_1} and G_{m_2,n_2} are given by Eq. (7) in the case of $\{m,n\} = \{m_1,n_1\}$ and $\{m,n\} = \{m_2,n_2\}$, respectively. Here we require the two SPDC processes to have the same signal frequency ω_s and the same idler frequency ω_i, with the energy-conservation condition $\omega_p = \omega_s + \omega_i$, where ω_p is the pump frequency. In addition, as we shall see in Sec. III, we require $m_1n_1 = \pm m_2n_2$. In order to show the experimental feasibility of such a structure, in the following we design two possible structures based on the temperature-dependent Sellmeier equation given by Emanueli and Arie [44].

We first design a structure for a degenerate source of $\lambda_p = 655$ nm, $\lambda_s = \lambda_i = 1310$ nm. Such a source could find applications in long-distance fiber-based quantum information

processing, as the wavelength of the photons is in the second telecom window. At a working temperature of 75 °C, we get the two reciprocals for QPM as $G_{3,1} = 17.47\ \mu\text{m}^{-1}$ and $G_{3,-1} = 18.24\ \mu\text{m}^{-1}$, corresponding to the two modulation periods $\Lambda_1 = 1.056\ \mu$m and $\Lambda_2 = 16.36\ \mu$m, respectively. The ratio of the two periods is $\Lambda_2/\Lambda_1 = 15.5$, and thus the duty cycle D_2 should be 15/31.

We design a second structure for a nondegenerate source of $\lambda_p = 532$ nm, $\lambda_s = 807.3$ nm, and $\lambda_i = 1560$ nm. This choice is motivated by the photon source requirements in real-world quantum networks, for example photonic memories in quantum repeaters. The shorter-wavelength photon of this source can be used for coupling and entangling atomic systems, and the other photon at 1560 nm can be transmitted over a long distance in fiber because its wavelength lies in the low-loss transmission window of optical fibers. By choosing the working temperature as 75.5 °C, we obtain the two reciprocals for QPM as $G_{3,1} = 14.95\ \mu\text{m}^{-1}$ and $G_{3,-1} = 15.93\ \mu\text{m}^{-1}$, with the two corresponding modulation periods as $\Lambda_1 = 1.220\ \mu$m and $\Lambda_2 = 12.82\ \mu$m, respectively, the ratio of which is $\Lambda_2/\Lambda_1 = 10.5$, and therefore the duty cycle $D_2 = 10/21$.

The above two example structures are both within current micron and submicron periodic poling techniques [45–47]. In the following section, we shall present the SPDC process in the DPPKTP crystal and study the performances of the two example sources.

III. GENERATION OF POLARIZATION-ENTANGLED PHOTONS

We consider a classical pump wave illuminating the DPPKTP crystal with a length of L in the x direction and the interaction volume denoted by V. The induced second-order nonlinear polarization is given by [48]

$$P_i^{(2)}(\vec{r},t) = \varepsilon_0 \chi_{ijk}^{(2)} E_j(\vec{r},t) E_k(\vec{r},t), \tag{12}$$

where ε_0 is the vacuum dielectric constant and $\chi_{ijk}^{(2)}$ is the second-order nonlinear susceptibility tensor, where i, j, k refer to the Cartesian components of the fields. Here, we use the Einstein notation of repeated indices for tensor products. The Hamiltonian of the electromagnetic system can be expressed as

$$H = \frac{1}{2}\int_V d^3\vec{r}\left(\vec{D}\cdot\vec{E} + \frac{1}{\mu_0}\vec{B}\cdot\vec{B}\right), \tag{13}$$

where μ_0 is the vacuum permeability constant. Since $\vec{D} = \varepsilon_0\vec{E} + \vec{P}$, we obtain the interaction Hamiltonian in the parametric down-conversion process,

$$\begin{aligned} H_I(t) &= \frac{1}{2}\int_V d^3\vec{r}\,\vec{P}\cdot\vec{E} \\ &= \varepsilon_0 \int_V d^3\vec{r}\,\chi^{(2)} E_p(\vec{r},t) E_s(\vec{r},t) E_i(\vec{r},t), \end{aligned} \tag{14}$$

where we replace $\chi_{ijk}^{(2)}/2$ with the second-order nonlinear susceptibility $\chi^{(2)}$ [48], which has the form of Eq. (8) for an ideal structure. After quantization of the electromagnetic fields, $E(\vec{r},t)$ becomes a Hilbert space operator $\hat{E}(\vec{r},t)$, which can be decomposed into its positive and negative parts $\hat{E}(\vec{r},t) = \hat{E}^{(+)}(\vec{r},t) + \hat{E}^{(-)}(\vec{r},t)$. Then we can rewrite the interaction Hamiltonians

$$\hat{H}_I(t) = \varepsilon_0 \int_V d^3\vec{r}\,\chi^{(2)}(x)\hat{E}_p^{(+)}(\vec{r},t)\hat{E}_s^{(-)}(\vec{r},t)\hat{E}_i^{(-)}(\vec{r},t) + \text{H.c.}, \tag{15}$$

where H.c. denotes the Hermitian conjugate part. Here, we only write the two terms that lead to energy-conserving processes, and we neglect the other six terms that do not satisfy energy conservation and are therefore of no importance in the steady state. Note that neglecting these contributions is equivalent to making the rotating-wave approximation.

Since the transverse structure of DPPKTP is homogeneous, we ignore the transverse vectors of interacting waves and only consider the interaction along the propagating direction. We consider the case of signal and idler photons in forward and backward directions, respectively. Then the negative parts of the field operators of the signal and idler $\hat{E}_s$, $\hat{E}_i$ are represented by Fourier integrals as

$$\hat{E}_s^{(-)}(x,t) = \sum_{q=H,V}\int d\omega_s E_{s,q}^* e^{-i(k_{s,q}x-\omega_s t)}\hat{a}_{s,q}^\dagger(\omega_s), \tag{16}$$

$$\hat{E}_i^{(-)}(x,t) = \sum_{q=H,V}\int d\omega_i E_{i,q}^* e^{i(k_{i,q}x+\omega_i t)}\hat{a}_{i,q}^\dagger(\omega_i), \tag{17}$$

where $E_{j,q} = i\sqrt{\hbar\omega_j/[4\pi\varepsilon_0 c n_q(\omega_j)]}$, $j = s,i$. For simplicity, here we consider a continuous-wave (cw) plane-wave pump with horizontal polarization. In addition, the pump field is treated as an undepleted classical wave, and thus the positive part of its field operator is replaced with its complex amplitude,

$$E_p^{(+)}(x,t) = E_p e^{i(k_{p,H}x-\omega_p t)}. \tag{18}$$

Then, by substituting Eqs. (8), (16), (17), and (18) into Eq. (15), we obtain

$$\begin{aligned} \hat{H}_I(t) = -\frac{\hbar E_P}{4\pi c}\sum_{q=H,V}\sum_{q'=H,V}\sum_{m,n} d\mathcal{G}_{m,n}\int_{-L}^{0} dx \int d\omega_s \\ \times \int d\omega_i \sqrt{\frac{\omega_s\omega_i}{n_q(\omega_s)n_{q'}(\omega_i)}}\hat{a}_{s,q}^\dagger(\omega_s)\hat{a}_{i,q'}^\dagger(\omega_i) \\ \times e^{i(\omega_s+\omega_i-\omega_p)t}e^{-i(k_{s,q}-k_{i,q'}-k_{p,H}+G_{m,n})x} + \text{H.c.} \end{aligned} \tag{19}$$

For the SPDC process, the interaction is weak, so under first-order perturbation theory the state evolution from time t' to t can be written as

$$|\Psi\rangle = |\text{vac}\rangle + \frac{1}{i\hbar}\int_{t'}^{t}\hat{H}_I(\tau)d\tau|\text{vac}\rangle. \tag{20}$$

Considering steady-state output, we may set $t' = -\infty$ and $t = \infty$. Then we have

$$\int_{-\infty}^{\infty} d\tau e^{i(\omega_s+\omega_i-\omega_p)\tau} = 2\pi\delta(\omega_s+\omega_i-\omega_p), \tag{21}$$

which gives the energy-conservation relation

$$\omega_s + \omega_i - \omega_p = 0. \tag{22}$$

The integral over crystal length can be calculated as

$$\int_{-L}^{0} dx\, e^{-i(k_{s,q}-k_{i,q'}-k_{p,H}+G_{m,n})x} = Lh(L\Delta k_{qq'}), \tag{23}$$

where $\Delta k_{qq'} = k_{p,H} - k_{s,q} + k_{i,q'} - G_{m,n}$ and the h function has the following form:

$$h(x) = \frac{1 - e^{-ix}}{ix} = e^{-i\frac{x}{2}} \operatorname{sinc} \frac{x}{2}. \tag{24}$$

$h(L\Delta k_{qq'})$ determines the natural bandwidth of the two-photon state, as we shall see. In the case of infinite crystal length, Eq. (23) becomes a δ function, thus leading to the momentum conservation, i.e., the perfect phase-matching condition, $\Delta k_{qq'} = 0$.

Suppose that perfect phase-matching conditions given by Eqs. (10) and (11) can be satisfied at frequencies Ω_s and Ω_i, with corresponding wave vectors $K_{s,H}$, $K_{s,V}$, $K_{i,H}$, and $K_{i,V}$, such that

$$\Omega_s + \Omega_i = \omega_p, \qquad K_{j,q} = \frac{n_q(\Omega_j)\Omega_j}{c}, \tag{25}$$

with $j = s,i$ and $q = H,V$. Due to the existence of the bandwidth, and constrained by Eq. (22), we let

$$\omega_s = \Omega_s + \nu, \qquad \omega_i = \Omega_i - \nu, \tag{26}$$

where $|\nu| \ll \Omega_j$, $j = s,i$. Then in the case of the QPM conditions given by Eqs. (10) and (11), we can write the state of SPDC as

$$\begin{aligned} |\Psi\rangle = |\text{vac}\rangle &+ A_{HV} d_{HV} L \int d\nu\, h(L\Delta k_{HV}) \hat{a}^\dagger_{s,H}(\Omega_s + \nu) \\ &\times \hat{a}^\dagger_{i,V}(\Omega_i - \nu)|\text{vac}\rangle + A_{VH} d_{VH} L \int d\nu\, h(L\Delta k_{VH}) \\ &\times \hat{a}^\dagger_{s,V}(\Omega_s + \nu)\hat{a}^\dagger_{i,H}(\Omega_i - \nu)|\text{vac}\rangle, \end{aligned} \tag{27}$$

where

$$d_{HV} = d\mathcal{G}_{m_1,n_1} = \frac{4d}{\pi^2 m_1 n_1} \sin\frac{m_1\pi}{2} \sin(n_1 D_2 \pi), \tag{28}$$

$$d_{VH} = d\mathcal{G}_{m_2,n_2} = \frac{4d}{\pi^2 m_2 n_2} \sin\frac{m_2\pi}{2} \sin(n_2 D_2 \pi), \tag{29}$$

$$A_{HV} = \frac{iE_p}{2c}\sqrt{\frac{\Omega_s\Omega_i}{n_{s,H}n_{i,V}}}, \tag{30}$$

$$A_{VH} = \frac{iE_p}{2c}\sqrt{\frac{\Omega_s\Omega_i}{n_{s,V}n_{i,H}}}, \tag{31}$$

with $n_{j,q}$ denoting the refraction index of a photon with polarization q at frequency Ω_j. Here $A_{HV}d_{HV}$ and $A_{VH}d_{VH}$ are slowly varying functions of frequency, which have been taken outside the integral.

We can see that the maximally polarization-entangled state can be obtained under the condition of $|A_{HV}d_{HV}h(L\Delta k_{HV})| = |A_{VH}d_{VH}h(L\Delta k_{VH})|$. The condition of $d_{HV} = d_{VH} = d'$ can be satisfied straightforwardly by choosing $m_1 n_1 = \pm m_2 n_2$. In the following, we make calculations on $h(L\Delta k_{HV})$ and $h(L\Delta k_{VH})$, i.e., the spectrum of the photon pairs. In other words, the two-photon correlation time is on the order of several hundred picoseconds.

A. Characterizing the spectrum of photon pairs generated from our source

We first expand the magnitudes of the wave vectors for signal and idler photons around the central frequencies Ω_s and Ω_i, respectively, up to first order in ν,

$$k_{s,q} = \frac{n_q(\omega_s)\omega_s}{c} \approx K_{s,q} + \frac{\nu}{u_q(\Omega_s)}, \tag{32}$$

$$k_{i,q} = \frac{n_q(\omega_i)\omega_i}{c} \approx K_{i,q} - \frac{\nu}{u_q(\Omega_i)}, \tag{33}$$

where $u_q(\Omega_j) = d\Omega_j/dK_{j,q}$ are the group velocities of signal and idler photons at central frequencies, with $j = s,i$ and $q = H,V$. Therefore, we obtain

$$\Delta k_{HV} = -\nu S_{HV}, \quad S_{HV} = \left[\frac{1}{u_H(\Omega_s)} + \frac{1}{u_V(\Omega_i)}\right], \tag{34}$$

$$\Delta k_{VH} = -\nu S_{VH}, \quad S_{VH} = \left[\frac{1}{u_V(\Omega_s)} + \frac{1}{u_H(\Omega_i)}\right]. \tag{35}$$

We thus obtain the joint spectral densities for the components $|H,V\rangle$ and $|V,H\rangle$,

$$|h(L\Delta k_{HV})|^2 = \operatorname{sinc}^2 \frac{\nu L S_{HV}}{2}, \tag{36}$$

$$|h(L\Delta k_{VH})|^2 = \operatorname{sinc}^2 \frac{\nu L S_{VH}}{2}, \tag{37}$$

and the corresponding bandwidths are $\Delta\omega_{HV} \approx 1.77\pi/(LS_{HV})$ and $\Delta\omega_{VH} \approx 1.77\pi/(LS_{VH})$, respectively. Compared with the usual forward-wave type-II SPDC under the same conditions on crystal length and frequencies [49], the backward-wave source has a much narrower bandwidth, with a reducing factor of $(u_H^{-1} + u_V^{-1})/|u_H^{-1} - u_V^{-1}|$.

More explicitly, we consider the two example structures given in Sec. II, and the crystal length is set to 2 cm. For the degenerate source, we get the bandwidth $\Delta\omega_{HV} = \Delta\omega_{VH} \approx 2\pi \times 3.66$ GHz and the reducing factor is 41. For the nondegenerate source, we obtain the two bandwidths as $\Delta\omega_{HV} \approx 2\pi \times 3.61$ GHz and $\Delta\omega_{VH} \approx 2\pi \times 3.63$ GHz, corresponding to reducing factors of 25.9 and 78.2, respectively. Note that, compared with the asymmetric spectrum in the forward-wave case, our backward-wave source has an almost symmetric spectrum.

B. Quantifying the polarization entanglement produced by our source

To quantify the polarization entanglement produced by our source, we employ a commonly used entanglement measure, namely concurrence [50], whose value ranges from 0 for a nonentangled state to 1 for a maximally entangled state. For a pure two-qubit state $|\psi\rangle$, expressed in a fixed basis such as $\{|00\rangle,|01\rangle,|10\rangle,|11\rangle\}$, the concurrence $C = |\langle\psi|\sigma_y \otimes \sigma_y|\psi\rangle|$, where σ_y is the second Pauli matrix $\left(\begin{smallmatrix} 0 & -i \\ i & 0 \end{smallmatrix}\right)$ in the same basis. For our source, we need to treat the two-photon term of the state given by Eq. (27), denoted as $|\Psi_2\rangle$. Note that the state $|\Psi_2\rangle$ is unnormalized, and the reciprocal of the square of its

normalization constant is the two-photon generation rate, given by

$$R = \langle\Psi_2|\Psi_2\rangle = d'^2L^2\left[|A_{HV}|^2\int dv|h(L\Delta k_{HV}(v))|^2 + |A_{VH}|^2\int dv|h(L\Delta k_{VH}(v))|^2\right]. \quad (38)$$

Substituting Eqs. (36) and (37) into the above equation, we obtain

$$R = 2\pi d'^2L\left(\frac{|A_{HV}|^2}{S_{HV}} + \frac{|A_{VH}|^2}{S_{VH}}\right). \quad (39)$$

Then we can calculate the concurrence

$$C = \frac{|\langle\Psi_2|\sigma_y\otimes\sigma_y|\Psi_2\rangle|}{\langle\Psi_2|\Psi_2\rangle} = \frac{d'^2L^2|A_{HV}A_{VH}|}{R}\left|\int dv\, h^*(L\Delta k_{HV}(v))h(L\Delta k_{VH}(v)) + \int dv\, h^*(L\Delta k_{VH}(v))h(L\Delta k_{HV}(v))\right|. \quad (40)$$

By substituting Eqs. (24), (34), and (35) into the above equation, we arrive at

$$C = \frac{2S_{\min}}{\delta_n S_{HV} + S_{VH}/\delta_n}, \quad (41)$$

where $S_{\min} = \min\{S_{HV}, S_{VH}\}$ and $\delta_n = \sqrt{n_{s,H}n_{i,V}/(n_{s,V}n_{i,H})}$.

For degenerate case, i.e., $\Omega_s = \Omega_i$, $S_{HV} = S_{VH}$, $\delta_n = 1$, and thus $C = 1$, so our source can generate degenerate maximal polarization entanglement. This feature can also be seen directly from the two-photon term of the state given by Eq. (27), which shows a maximally entangled state in the form of $(|HV\rangle + |VH\rangle)/\sqrt{2}$.

While for non-degenerate case, i.e., $\Omega_s \neq \Omega_i$, $S_{HV} \neq S_{VH}$, $\delta_n \neq 1$, and therefore $C < 1$, so the entanglement is nonmaximal. However, actually there is not a big difference between $\delta_n S_{HV}$ and S_{VH}/δ_n, so the concurrence is very near to 1. Explicitly, let us consider the example structure given in Sec. II, the concurrence of the entanglement generated from which is found to be as high as 0.9978.

C. Generation rate of the entangled photon pairs

The photon pair generation rate can be estimated from Eq. (39) by substituting Eqs. (30), (31), and $|E_p|^2 = 2P/(\varepsilon_0 n_p c S)$ into it, where P denotes the pump power and S represents the transverse area of the pump beam. Therefore, we obtain

$$R = \frac{\pi d'^2 L P\Omega_s\Omega_i}{\varepsilon_0 n_p c^3 S}\left(\frac{1}{n_{s,H}n_{i,V}S_{HV}} + \frac{1}{n_{s,V}n_{i,H}S_{VH}}\right). \quad (42)$$

Let us consider the two specific example sources, for which we set $P = 1$ mW, $S = 0.01$ mm^2, and $L = 2$ cm. The nonlinear coefficient d' is given by Eq. (28), where $m_1 = 3$, $n_1 = 1$, and the effective nonlinear coefficient d, stemming from d_{24}, is found to be 3.9 pm/V. Then we find the generation rate of the degenerate source to be 421 pairs/s, and thus we get the spectral brightness as $2\pi R/\Delta\omega \approx 115$ pairs/(s GHz mW). The generation rate of the nondegenerate source is found to be 554 pairs/s, corresponding to the spectral brightness of 154 pairs/(s GHz mW). We have to emphasize that the experimental value of the photon pair rate and the two-photon spectrum will definitely be affected by the poling quality, e.g., the deviations and fluctuation of the poling period and duty cycle [51]. However, the state of the art of the poling technique can enable us to engineer a nearly idealized poled structure.

IV. CONCLUSIONS

In conclusion, we have presented a scheme for building polarization-entangled photon pair sources utilizing backward-wave-type SPDC processes in a dual-periodically-poled crystal. Our scheme does not rely on any state projection and can work in degenerate and nondegenerate cases. The backward-wave-type SPDC enables the entangled photon pairs from our source to transmit in a beamlike way, exhibiting more efficient photon collection and mode overlapping. Furthermore, the backward-wave-type SPDC has a much narrower bandwidth than the usual forward-wave one. In addition, our scheme employs two concurrent SPDC processes in a single crystal rather than any interferometer, and therefore our source is compact and stable. By proper engineering on the domain structure, a complete set of Bell states can be achieved directly from this DPPKTP crystal [52]. This implies further applications in integrated photonic quantum technologies.

We have designed two possible DPPKTP structures for degenerate and nondegenerate sources, respectively. Using a 2-cm-long bulk crystal, the bandwidths of the two sources were found to be ~3.6 GHz with spectral brightnesses of 115 and 154 pairs/(s GHz mW), respectively. Our high-spectral-brightness narrow-band sources should find applications in large-scale quantum networks and other fields requiring narrow-band entangled photons. Furthermore, we have also quantified the polarization entanglement via concurrence and found that the degenerate source can provide maximally polarization-entangled photon pairs while the concurrence of the polarization entanglement generated from the nondegenerate source is as high as 0.9978. Finally, the two structures are both within current manufacture technologies, and thus we believe our sources can be realized in experiment. We hope our approach can stimulate more investigations on applications of QPM on photonic quantum technologies.

ACKNOWLEDGMENTS

Y.X.G. thanks Bao-Sen Shi and Xu-Bo Zou for stimulating discussions. This work was supported by the National Natural Science Foundation of China (Grant Nos. 11004096, 10904066, 11004030, 11004029, and 11174052), and the State Key Program for Basic Research of China (Grant Nos. 2011CBA00205 and 2012CB921802).

[1] M. Genovese, Phys. Rep. **413**, 319 (2005).
[2] J. L. O'Brien, A. Furusawa, and J. Vučković, Nat. Photon. **3**, 687 (2009).
[3] P. G. Kwiat, K. Mattle, H. Weinfurter, A. Zeilinger, A. V. Sergienko, and Y. Shih, Phys. Rev. Lett. **75**, 4337 (1995).
[4] P. G. Kwiat, E. Waks, A. G. White, I. Appelbaum, and P. H. Eberhard, Phys. Rev. A **60**, R773 (1999).
[5] Y.-H. Kim, S. P. Kulik, and Y. Shih, Phys. Rev. A **63**, 060301 (2001).
[6] J. A. Armstrong, N. Bloembergen, J. Ducuing, and P. S. Pershan, Phys. Rev. **127**, 1918 (1962).
[7] P. A. Franken and J. F. Ward, Rev. Mod. Phys. **35**, 23 (1963).
[8] S. Tanzilli, H. D. Riedmatten, W. Tittel, H. Zbinden, P. Baldi, M. D. Micheli, D. Ostrowsky, and N. Gisin, Electron. Lett. **37**, 26 (2001).
[9] A. Yoshizawa and H. Tsuchida, Appl. Phys. Lett. **85**, 2457 (2004).
[10] F. König, E. J. Mason, F. N. C. Wong, and M. A. Albota, Phys. Rev. A **71**, 033805 (2005).
[11] Y.-K. Jiang and A. Tomita, J. Phys. B **40**, 437 (2007).
[12] H. C. Lim, A. Yoshizawa, H. Tsuchida, and K. Kikuchi, Opt. Express **16**, 12460 (2008); **16**, 16052 (2008).
[13] S. Sauge, M. Swillo, M. Tengner, and A. Karlsson, Opt. Express **16**, 9701 (2008).
[14] M. Hentschel, H. Hübel, A. Poppe, and A. Zeilinger, Opt. Express **17**, 23153 (2009).
[15] M. Fiorentino and R. G. Beausoleil, Opt. Express **16**, 20149 (2008).
[16] E. V. Moreva, G. A. Maslennikov, S. S. Straupe, and S. P. Kulik, Phys. Rev. Lett. **97**, 023602 (2006).
[17] M. Pelton, P. Marsden, D. Ljunggren, M. Tengner, A. Karlsson, A. Fragemann, C. Canalias, and F. Laurell, Opt. Express **12**, 3573 (2004).
[18] D. Ljunggren, M. Tengner, P. Marsden, and M. Pelton, Phys. Rev. A **73**, 032326 (2006).
[19] T. Suhara, G. Nakaya, J. Kawashima, and M. Fujimura, IEEE Photon. Technol. Lett. **21**, 1096 (2009).
[20] K. Thyagarajan, J. Lugani, S. Ghosh, K. Sinha, A. Martin, D. B. Ostrowsky, O. Alibart, and S. Tanzilli, Phys. Rev. A **80**, 052321 (2009).
[21] Z. H. Levine, J. Fan, J. Chen, and A. L. Migdall, Opt. Express **19**, 6724 (2011).
[22] N. Gisin and R. Thew, Nat. Photon. **1**, 165 (2007).
[23] P. Kok, W. J. Munro, K. Nemoto, T. C. Ralph, J. P. Dowling, and G. J. Milburn, Rev. Mod. Phys. **79**, 135 (2007).
[24] C. E. Kuklewicz, M. Fiorentino, G. Messin, F. N. C. Wong, and J. H. Shapiro, Phys. Rev. A **69**, 013807 (2004).
[25] M. Fiorentino, G. Messin, C. E. Kuklewicz, F. N. C. Wong, and J. H. Shapiro, Phys. Rev. A **69**, 041801 (2004); T. Kim, M. Fiorentino, and F. N. C. Wong, *ibid.* **73**, 012316 (2006); O. Kuzucu and F. N. C. Wong, *ibid.* **77**, 032314 (2008).
[26] A. Fedrizzi, T. Herbst, A. Poppe, T. Jennewein, and A. Zeilinger, Opt. Express **15**, 15377 (2007).
[27] M. Halder, S. Tanzilli, H. de Riedmatten, A. Beveratos, H. Zbinden, and N. Gisin, Phys. Rev. A **71**, 042335 (2005).
[28] L.-M. Duan, M. D. Lukin, J. I. Cirac, and P. Zoller, Nature (London) **414**, 413 (2001).
[29] H. de Riedmatten, M. Afzelius, M. U. Staudt, C. Simon, and N. Gisin, Nature (London) **456**, 773 (2008).
[30] K. F. Reim, J. Nunn, V. O. Lorenz, B. J. Sussman, K. C. Lee, N. K. Langford, D. Jaksch, and I. A. Walmsley, Nat. Photon. **4**, 218 (2010).
[31] M. Halder, A. Beveratos, N. Gisin, V. Scarani, C. Simon, and H. Zbinden, Nat. Phys. **3**, 692 (2007).
[32] Z. Y. Ou and Y. J. Lu, Phys. Rev. Lett. **83**, 2556 (1999).
[33] X.-H. Bao, Y. Qian, J. Yang, H. Zhang, Z.-B. Chen, T. Yang, and J.-W. Pan, Phys. Rev. Lett. **101**, 190501 (2008).
[34] M. Scholz, L. Koch, and O. Benson, Phys. Rev. Lett. **102**, 063603 (2009).
[35] A. Christ, A. Eckstein, P. J. Mosley, and C. Silberhorn, Opt. Express **17**, 3441 (2009).
[36] T. Suhara and M. Ohno, IEEE J. Quantum Electron. **46**, 1739 (2010).
[37] C.-S. Chuu and S. E. Harris, Phys. Rev. A **83**, 061803 (2011).
[38] A. De Rossi and V. Berger, Phys. Rev. Lett. **88**, 043901 (2002).
[39] M. C. Booth, M. Atatüre, G. Di Giuseppe, B. E. A. Saleh, A. V. Sergienko, and M. C. Teich, Phys. Rev. A **66**, 023815 (2002); Z. D. Walton, M. C. Booth, A. V. Sergienko, B. E. A. Saleh, and M. C. Teich, *ibid.* **67**, 053810 (2003); Z. D. Walton, A. V. Sergienko, B. E. A. Saleh, and M. C. Teich, *ibid.* **70**, 052317 (2004).
[40] J. Perina Jr., Phys. Rev. A **77**, 013803 (2008).
[41] M. Ravaro, Y. Seurin, S. Ducci, G. Leo, V. Berger, A. De Rossi, and G. Assanto, J. Appl. Phys. **98**, 063103 (2005); L. Lanco, S. Ducci, J.-P. Likforman, X. Marcadet, J. A. W. van Houwelingen, H. Zbinden, G. Leo, and V. Berger, Phys. Rev. Lett. **97**, 173901 (2006); A. Orieux, X. Caillet, A. Lemaître, P. Filloux, I. Favero, G. Leo, and S. Ducci, J. Opt. Soc. Am. B **28**, 45 (2011).
[42] M. H. Chou, K. R. Parameswaran, M. M. Fejer, and I. Brener, Opt. Lett. **24**, 1157 (1999).
[43] Z.-W. Liu, Y. Du, J. Liao, S.-N. Zhu, Y.-Y. Zhu, Y.-Q. Qin, H.-T. Wang, J.-L. He, C. Zhang, and N.-B. Ming, J. Opt. Soc. Am. B **19**, 1676 (2002).
[44] S. Emanueli and A. Arie, Appl. Opt. **42**, 6661 (2003).
[45] C. Canalias, V. Pasiskevicius, R. Clemens, and F. Laurell, Appl. Phys. Lett. **82**, 4233 (2003).
[46] C. Canalias, V. Pasiskevicius, M. Fokine, and F. Laurell, Appl. Phys. Lett. **86**, 181105 (2005).
[47] C. Canalias and V. Pasiskevicius, Nat. Photon. **1**, 459 (2007).
[48] R. W. Boyd, *Nonlinear Optics*, 2nd ed. (Academic, San Diego, CA, 2003).
[49] M. H. Rubin, D. N. Klyshko, Y. H. Shih, and A. V. Sergienko, Phys. Rev. A **50**, 5122 (1994).
[50] S. Hill and W. K. Wootters, Phys. Rev. Lett. **78**, 5022 (1997); W. K. Wootters, *ibid.* **80**, 2245 (1998).
[51] M. Fejer, G. Magel, D. Jundt, and R. Byer, IEEE J. Quantum Electron. **28**, 2631 (1992).
[52] H. Guillet de Chatellus, A. V. Sergienko, B. E. A. Saleh, M. C. Teich, and G. Di Giuseppe, Opt. Express **14**, 10060 (2006).